PRELIMINARY IMPEDANCE BUDGET FOR THE TPS STORAGE RING

A. Rusanov*, NSRRC, Hsinchu 30076, Taiwan, R.O.C.

Abstract

The Taiwan Photon Source (TPS) is a new 3 GeV third generation synchrotron storage ring which will be built at the present site of the National Synchrotron Radiation Research Center in Hsinchu, Taiwan. Preliminary results of ongoing impedance studies of storage ring vacuum components for the TPS project are presented in the paper. Wakes and impedances produced by each component of the storage ring have been evaluated by using a 3D electromagnetic code. Threshold current of the longitudinal microwave instability is estimated.

INTRODUCTION

Single bunch current in the storage ring should be below threshold of the longitudinal microwave instability arising from the interaction of a bunch with itself via short-range wake fields. Short-range wake, in its turn, defines broad-band impedance and hence maximum value of the single bunch current depends mainly on the broad-band impedance. The overall impedance of the vacuum chamber should be carefully evaluated to estimate threshold current of the longitudinal microwave instability, which can lead to bunch lengthening.

NUMERICAL CODE AND TECHNIQUES

A 3D electromagnetic field simulator GdfidL [1] was used to study wakes in the TPS storage ring. Common parameters for GdfidL computations for all the structures described in the report are summarized in Table 1.

Table 1: Parameters for GdfidL computations

Parameter	Value
Mesh size	0.25×10^{-3}m
Bunch shape	Gaussian
RMS bunch length σ_s	3.0×10^{-3}m
Distance from bunch s	1.0m

For structures with resonance behavior of electromagnetic fields, such as cavities or flanges, a longer distance from bunch was considered. Bigger transverse mesh size was considered for structures with big geometrical dimensions, for example, cavities.

Stereolithography (STL) files were used as GdfidL input data for most of the TPS storage ring components. Wakes, impedances, loss factors for each component were obtained as a result of the simulations.

* rusanov@nsrrc.org.tw

The type of wake produced by a component (capacitive, resistive or inductive) can be distinguished from its behavior at very short range after the start of the bunch. Once classified, an analytic expression [2, 3] can be used to relate the maximum of the wake from a bunch to the broad-band impedance Z/n, where $n = \omega/\omega_0$ and ω_0 is the revolution frequency.

The longitudinal microwave instability was studied with numerical code ZAP [4].

STORAGE RING COMPONENTS

Beam position monitors, bellows, cavities, flanges, photon absorbers, pumping slots chambers, and several kinds of tapers were simulated so far. Fig. 1 shows wakes from several groups of elements as well as the total wake. One can see that the biggest wakes are produced by bellows and tapers.

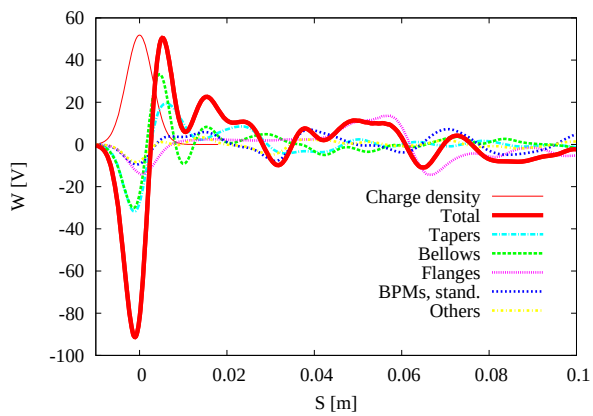

Figure 1: Longitudinal wake as a function of distance from bunch for various groups of elements.

Most of the components studied in the paper are common and have been used in many storage rings. Nevertheless, some studies were performed in order to optimize impedance of components and to clarify dependence of the impedance on the geometry of components.

There should be more than two hundreds photon absorbers with different heights installed in the ring. Dependences of impedance and loss factors on absorbers' height were studied showing that higher absorbers cause bigger broad-band impedance and loss factors. This dependence has an almost linear shape.

Titanium bellows are proposed for the TPS storage ring. Radio frequency (RF) shielding of bellows has long slot in its solid part. Two types of bellows were studied: with two

such slots and with only one slot. Results of simulations show that there is only minor difference in the shape of wakes from bellows with two and one slot. This means that the contribution to the impedance from longitudinal slots in the RF shielding is insignificant.

Wake produced by the TPS flange systems has fast oscillations along the pipe axis. This happens because electron bunch excites resonant modes in the gap between flanges and electromagnetic field can store significant amount of energy in the structure. Even with RF shielding present, the gap between flanges represents a very narrow cylindrical cavity of complicated geometry. However, it was confirmed that even the lowest resonance mode is not trapped in such a cavity and has a low quality factor.

A Superconducting RF (SRF) cavity designed by Cornell University is proposed for the TPS storage ring. SRF cavity and cavity tapers (transition from circular to elliptical cross-section) were simulated separately. Only the fundamental mode of the cavity has high quality factor and hence high impedance. The rest of the modes have low quality factors due to energy leakage to the beam pipes. Wake fields produced by the cavity tapers are rather big. This results in relatively high broad-band impedance of this structure.

There are several kinds of tapers proposed for the TPS storage ring besides SRF cavity tapers: injection section tapers, tapers for both sides of long straight sections, tapers for insertion devices (ID) chambers. ID chambers were studied in detail, because this kind of elements is one of the major contributors to the broad-band impedance of the storage ring. Tapered structures of TPS ID chambers were simulated in GdfidL assuming different dimensions of the beam-pipe with race-track cross-section (narrow part). Results of simulations show that dependences of the loss factor and broad-band impedance on the width of the beam pipe with race track cross-section are almost linear. The smaller is the gap of the ID chamber the higher are its loss factor and impedance. In the final design, the slope of the tapers should be chosen with care to meet the broad-band impedance goals of the ring.

IMPEDANCE BUDGET

Figs. 2 and 3 display the frequency content of the longitudinal coupling impedance. It is seen that tapers contribute to the impedance mainly in the frequency ranges 5–20GHZ (real part) and 5GHz (imaginary part), bellows significantly enhance impedance in the frequency ranges 20–30GHZ (real part) and 10–30GHz (imaginary part). BPMs and flanges are responsible for numerous peaks of impedance in both real and imaginary parts. Impedance of the SRF cavity is localized in the frequency range 500MHz.

A preliminary impedance budget for the TPS storage ring is shown in Table 2, where longitudinal broad-band impedance $|Z_\parallel/n|$, longitudinal loss factor $k_\parallel$, transverse kick factors k_x, k_y, and estimated number of elements in the ring N are presented. The total longitudinal broad-band

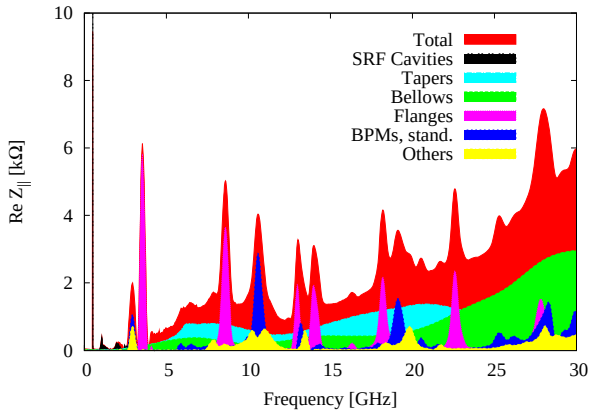

Figure 2: Frequency content of the longitudinal coupling impedance (real part).

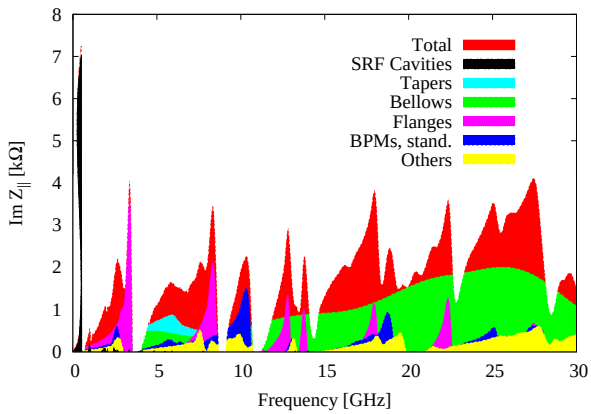

Figure 3: Frequency content of the longitudinal coupling impedance (imaginary part).

impedance calculated thus far is 0.36Ω.

Fig. 4 shows contributions to the total longitudinal broad-band impedance and total longitudinal loss factor from different groups of elements. One can see that major contributors to the total longitudinal impedance are SRF cavities, flanges, and bellows. Major contributors to the total longitudinal loss factor are flanges, bellows, and SRF cavity tapers.

INSTABILITY THRESHOLD

Total value of the longitudinal broad-band impedance was used to study the longitudinal microwave instability in the TPS storage ring. Potential well distortion was taken into account. Result of simulations is presented in Fig. 5. From this figure one can see that with increasing bunch current its length becomes smaller and only above some threshold current there is a rather fast bunch lengthening. The result obtained shows that nominal designed single bunch current of the TPS storage 0.67A is below threshold of the longitudinal microwave instability.

Table 2: Preliminary impedance budget for the TPS storage ring

Components	$\lvert Z_{\parallel}/n\rvert$, Ω	$k_{\parallel}$, V/pC	k_x, $V/pC/m$	k_y, $V/pC/m$	N
Σ Absorbers (injection section)	9.27×10^{-6}	1.36×10^{-3}	4.79×10^{-2}	4.99×10^{-11}	1
Σ Absorbers (straight sections)	3.62×10^{-5}	6.42×10^{-3}	1.78×10^{-1}	6.71×10^{-11}	24
Bellows (straight sections)	3.14×10^{-4}	6.12×10^{-2}	7.53×10^{-3}	1.99×10^{-1}	144
BPM, primary (long straight sections)	1.72×10^{-4}	6.39×10^{-2}	1.26×10^{-5}	1.95×10^{-6}	48
BPM, standard (achromatic sections)	8.50×10^{-5}	3.35×10^{-2}	1.24×10^{-3}	9.00×10^{-4}	168
Flange (straight sections)	3.57×10^{-4}	5.82×10^{-2}	2.57×10^{-4}	3.15×10^{-4}	168
Pumping slots chamber (straight sections)	1.36×10^{-5}	1.17×10^{-3}	2.53×10^{-10}	1.37×10^{-11}	96
SRF Cavity (500MHz)	4.49×10^{-2}	3.94×10^{-1}	1.66×10^{-6}	1.66×10^{-6}	4
SRF Cavity Tapers	8.07×10^{-3}	3.68	1.56×10^{-1}	2.78×10^{-5}	2
Taper (injection section)	2.66×10^{-5}	1.19×10^{-2}	3.08×10^{-1}	7.97×10^{-13}	1
Taper (straight sections)	5.29×10^{-4}	9.67×10^{-2}	8.99×10^{-3}	6.40×10^{-2}	48
Taper, ID (straight sections)	2.37×10^{-3}	6.92×10^{-1}	1.49×10^{-7}	2.83×10^{-7}	4

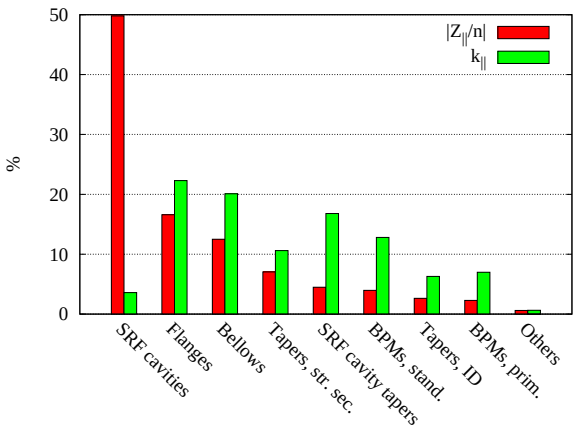

Figure 4: Contributions to the total longitudinal broad-band impedance and total longitudinal loss factor from different groups of elements.

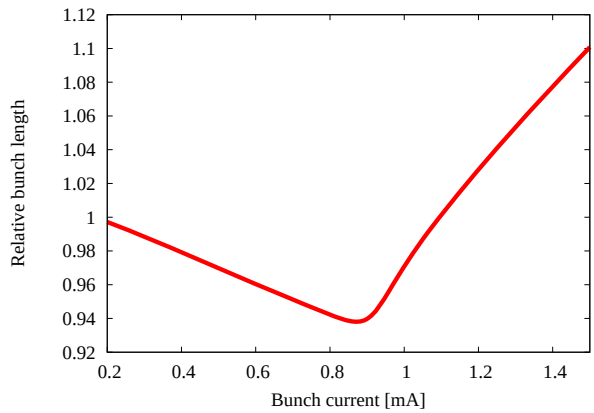

Figure 5: Dependence of the relative bunch length on single bunch current obtained with ZAP.

The most accurate result for threshold of the longitudinal microwave instability can be obtained from tracking codes using the total wake field from all the components in the storage ring.

CONCLUSIONS

The TPS storage ring broad-band impedance and loss factor have been calculated. Contributions to the total longitudinal broad-band impedance and total longitudinal loss factor from different groups of elements were found. Frequency content of the total longitudinal coupling impedance was studied, and major contributors in different frequency ranges were determined. It is confirmed that nominal single bunch current of the storage ring is below threshold of the longitudinal microwave instability.

ACKNOWLEDGMENTS

I would like to thank P.-J. Chou, C.-C. Kuo, Ch. Wang (NSRRC), A. Blednykh (BNL), and R. Nagaoka (SOLEIL) for their help and discussions on GdfidL use and obtained results. Thanks to G.-Y. Hsiung and other colleagues of the NSRRC vacuum group for providing detailed information on vacuum chambers. I also thank H. Wiedemann (Stanford University) for his comments on the results presented here.

REFERENCES

[1] W. Bruns, “The GdfidL Electromagnetic Field Simulator”, http://gdfidl.de.

[2] R.T. Dowd, M.J. Boland, G.S. LeBlanc, M.J. Spencer, Y.-R.E. Tan, “Impedance and Beam Stability Study at the Australian Synchrotron”, Proc. of EPAC’06 Conference, June 2006, Edinburgh, Scotland.

[3] F. Pérez, “Impedance, Loss Factor and Beam Stability Calculations for the ANKA Storage Ring”, Proc. of EPAC’98 Conference, June 1998, Stockholm, Sweden.

[4] M.S. Zisman, S. Chattopadhyay, J.J. Bisognano, “ZAP User’s Manual”, LBL-21270, ESC-15, 1986.